Pathology - Research and Practice 251 (2023) 154901

Contents lists available at ScienceDirect

Pathology - Research and Practice

journal homepage: www.elsevier.com/locate/prp

PTX3 shapes profibrotic immune cells and epithelial/fibroblast repair and regeneration in a murine model of pulmonary fibrosis

Antonio d'Amati [a,b], Roberto Ronca [c], Federica Maccarinelli [c], Marta Turati [c], Loredana Lorusso [a], Michelina De Giorgis [a], Roberto Tamma [a], Domenico Ribatti [a], Tiziana Annese [a,d,*]

[a] Department of Basic Medical Sciences, Neurosciences and Sensory Organs, University of Bari Medical School, Bari, Italy
[b] Section of Pathology, Department of Emergency and Organ Transplantation, University of Bari, 70124 Bari, Italy
[c] Department of Molecular and Translational Medicine, School of Medicine, University of Brescia, 25123 Brescia, Italy
[d] Department of Medicine and Surgery, LUM University, Casamassima, 70010 Bari, Italy

ARTICLE INFO

Keywords:
CD44
Immune cells
Long pentraxin-3
Macrophages
Mast cells
Pulmonary fibrosis
Regeneration
T cells
SOX2

ABSTRACT

The long pentraxin 3 (PTX3) is protective in different pathologies but was not analyzed in-depth in Idiopathic Pulmonary Fibrosis (IPF). Here, we have explored the influence of PTX3 in the bleomycin (BLM)-induced murine model of IPF by looking at immune cells (macrophages, mast cells, T cells) and stemness/regenerative markers of lung epithelium (SOX2) and fibro-blasts/myofibroblasts (CD44) at different time points that retrace the progression of the disease from onset at day 14, to full-blown disease at day 21, to incomplete regression at day 28. We took advantage of transgenic PTX3 overexpressing mice (Tie2-PTX3) and Ptx3 null ones (PTX3-KO) in which pulmonary fibrosis was induced. Our data have shown that PTX3 overexpression in Tie2-PTX3 compared to WT or PTX3-KO: reduced $CD68^+$ and $CD163^+$ macrophages and the $Tryptase^+$ mast cells during the whole experimental time; on the contrary, $CD4^+$ T cells are consistently present on day 14 and dramatically decreased on day 21; $CD8^+$ T cells do not show significant differences on day 14, but are significantly reduced on day 21; SOX2 is reduced on days 14 and 21; CD44 is reduced on day 21. Therefore, PTX3 could act on the proimmune and fibrogenic microenvironment to prevent fibrosis in BLM-treated mice.

1. Introduction

Idiopathic Pulmonary Fibrosis (IPF) is a chronic interstitial lung disease in which diffuse scar tissue progressively affects the lungs, making breathing increasingly harder [1]. IPF usually presents around 70–75 years old, is rare in people under 50, the distribution is global, the incidence is increasing, and poor is the long-term prognosis (>50% of the patients die within 3 years after diagnosis) [1,2].

IPF etiology is unknown, but tobacco smoke [3,4], metal dust [5], wood dust [6], pesticides [7], and gastroesophageal reflux [8] have been identified as environmental and behavioral risk factors. IPF familial cases were related to genetic risk factors such as mutations in the telomerase, surfactant and mucin genes [9,10]. The diagnosis can be made by computed tomography (CT) scan and/or by lung biopsy, which will respectively show a characteristic imaging or histological pattern of "usual interstitial pneumonia" (UIP) [11–13]. There is currently no cure for IPF, but several palliative treatments include self-care measures, oxygen supplementation, antifibrotic drugs, and lung transplants for severe diseases [14].

In IPF, at the microscopic examination, the pulmonary tissue presents scar tissue characterized by progressive fibrosis due to failed alveolar reepithelialization and fibroblast/myofibroblast accumulation (known as fibroblastic foci), hyperplasia of alveolar epithelial cells and fibroblasts, deposition of extracellular matrix, and proliferation of inflammatory cells in the interstitial and alveolar spaces [15,16].

Inflammation is not a main histopathological finding in IPF [15,17]. However, immune cells infiltrate the fibrotic lung [18,19], and their characterization could be helpful in investigating the etiopathogenesis of IPF. Among the regulators, soluble regulators of innate immunity, the long pentraxin 3 (PTX3) seems to exert a protective role in IPF, as demonstrated in the bleomycin (BLM)-induced experimental model of lung fibrosis [20].

PTX3 is a member of soluble pattern recognition receptors (sPRR) rapidly produced by several cell types [21] in response to fungi [22], bacteria [23,24] and viruses [25]. PTX3 is a humoral mediator of innate immunity [26], and its concentration is low in tissue and serum under

* Corresponding author at: Department of Basic Medical Sciences, Neurosciences and Sensory Organs, University of Bari Medical School, Bari, Italy.
E-mail address: annese@lum.it (T. Annese).

https://doi.org/10.1016/j.prp.2023.154901
Received 29 August 2023; Received in revised form 11 October 2023; Accepted 19 October 2023
Available online 20 October 2023

physiological conditions [27]. It acts as an opsonin during infections, facilitates recognition and phagocytosis by macrophages [28], activates the complement cascade [29,30], and orchestrates tissue repair playing non-redundant roles [31,32]. In tissue damage models, the lack of PTX3 was associated with altered turnover of fibrin-rich deposits, followed by increased collagen deposition [33]. However, it is important to note that PTX3, as the other related pentraxins C-reactive protein (CRP) and serum amyloid P (SAP), can also amplify tissue damage [34,35].

Several studies have shown a potential protective role of PTX3 in different lung pathologies, such as in: mouse orthotopic lung transplantation model in which increased lung fibrosis is present in PTX3-KO mice [36]; cecal ligation and puncture-induced sepsis murine model after ethanol/saline administration, in which PTX3 suppression contribute to sepsis exacerbation [37]; mouse neonates Pseudomonas aeruginosa infection in which orally administered PTX3 protected against lung infection [38].

The most characterized animal model of IPF available and relevant for the preclinical test is the intratracheal BLM-induced murine model [39,40]. In this murine model, PTX3 has been demonstrated to protect mice from BLM-induced pulmonary fibrosis because PTX3 is expressed at fibroblastic foci, and its distribution was related to collagen deposition, reduced fibroblast activation, and decreased immune infiltrate [20,41,42].

In the present study, we started with the animal employed and data obtained in the work of Maccarinelli et al. [20] to investigate the impact of PTX3 in the BLM-induced murine model of IPF. We have examined, at different time points, the pulmonary microenvironment by looking at immune cell infiltrate (macrophages, mast cells, T cells) and stemness/regenerative markers of lung epithelium (SOX2) and fibroblasts/myofibroblasts (CD44). We used transgenic PTX3 overexpressing mice (Tie2-PTX3) and Ptx3 null ones (PTX3-KO), in which pulmonary fibrosis was induced by intratracheal bleomycin instillation. Our data show that: throughout the whole experimental period, the $CD68^+$ and $CD163^+$ macrophages and the $Tryptase^+$ mast cells are reduced in the Tie2-PTX3 pulmonary microenvironment compared to wild-type (WT) or PTX3-KO; on the contrary, $CD4^+$ T cells are consistently present on day 14 and dramatically decreased on day 21 in Tie2-PTX3 compared to WT or PTX3-KO; $CD8^+$ T cells do not show significant differences on day 14, but are amply reduced on day 21 in Tie2-PTX3 compared to WT or PTX3-KO; SOX2 is reduced on days 14 and 21 in Tie2-PTX3 compared to WT or PTX3-KO; CD44 is reduced on day 21 in Tie2-PTX3 compared to WT or PTX3-KO. Moreover, statistical correlation has shown a positive and very strong correlation between CD44 and CD8 expression, while moderate was the correlation between CD44 and Tryptase and between SOX2 and CD8. This scenario confirmed the effects of PTX3 on the progression of IPF. However, it provided new insight into PTX3's role during disease progression on mast cells, T cells, lung epithelium and fibroblasts/myofibroblasts, demonstrating a pivotal role of PTX3, which reduces the amount of these cells that could act as profibrotic cells during pulmonary fibrosis.

2. Materials and methods

2.1. Biological samples

The lungs for histopathological analysis from wild-type (WT) C57BL/6 mice (n = 6), transgenic mice overexpressing PTX3 in endothelial cells and stroma (Tie2-PTX3) (n = 6) and knockout mice lacking the Ptx3 gene in homozygosis (PTX3-KO) (n = 4) [43,44], were obtained from 8 weeks old male mice appropriately treated to induce pulmonary fibrosis by a single slow intratracheal injection of 4.0 mg/kg bleomycin (B2434 Sigma-Aldrich) dissolved in 30 μl of phosphate-buffered saline (PBS). Afterward, mice were sacrificed at 14, 21, and 28 days after injection, and the pulmonary fibrosis areas were evaluated by Masson's trichrome staining quantification of fibrotic/collagen positive areas and by hydroxyproline quantification as a marker for the presence of collagen in the ECM, as in-depth described elsewhere [20].

Pulmonary fibrosis was found in WT mice from day 14 (onset) to day 21 (the peak), with an incomplete regression at day 28 (see Fig. 2 in [20]). In the same study with the same mice, it was observed that PTX3 expression increased in WT BLM-treated mice at fibrotic lesions on day 14 and decreased to day 0 levels on day 28 (see Fig. 1 in [20]). On the contrary, in Tie2-PTX3 mice, no significant variations in amount were found among the different time points (see figure S2 in [20]).

2.2. Immunohistochemistry

Four-micrometer-thick, 10% formalin-fixed and paraffin-embedded histological sections were deparaffinized and rehydrated in a xylene-graded alcohol scale, rinsed in Tris-buffered saline solution (TBS), and treated with blocker for endogenous peroxidase and phosphatase enzymes (S2003, Agilent Dako).

Immunostaining was performed upon thermostatic water bath epitope retrieval (30 min, 98 °C) in sodium citrate pH 6.0 buffer (S1699, Agilent Dako) for all the primary antibodies.

For CD4, CD8, CD68, CD163, SOX2 and CD44 immunolabelling, the following primary antibodies, diluted in antibody diluent (ab64211, Abcam), were employed: rabbit polyclonal anti-CD44 (ab189524, Abcam; diluted 1:4000), rabbit polyclonal anti-CD8 (ab203035, Abcam; diluted 1:400), rabbit polyclonal anti-CD68 (ab125047, Abcam; diluted 1:100), rabbit polyclonal anti-CD163 (ab182422, Abcam; diluted 1:500); rabbit polyclonal anti-SOX2 (ab92494, Abcam; diluted 1:80), and rabbit polyclonal anti-CD44 (ab189524, Abcam; diluted 1:4000). After primary antibody exposition step for 1 h at room temperature, the sections were incubated with biotinylated polymer, the streptavidin-alkaline phosphatase for 15 min each and the red chromogen for 20 min (all from K5005, Agilent Dako) for signal detection.

For Tryptase immunolabeling [45], the sections were primarily incubated with a rodent block (ab127055, Abcam) for 30 min at room temperature, exposed to mouse monoclonal-Tryptase (ab2378, Abcam; diluted 1:250) for 1 h at room temperature, incubated with the mouse on mouse polymer for IHC (ab127055, Abcam) for 15 min, and the immunodetection was performed with DAB substrate kit (SK-4100, Vector Laboratories) for peroxidase signal detection.

All the sections were counterstained with Gill's hematoxylin (51275, Sigma-Aldrich) and mounted in glycergel (C0563, Agilent Dako). Negative controls were provided by specific preimmune serums that replaced the primary antibodies.

2.3. Morphometric analysis

Immunolabeled slides were digitalized using the whole-slide scanning platform Aperio ScanScope CS (Leica Biosystems) at 40x magnification, stored by the management system Aperio eSlide Manager (Leica Biosystems), and analyzed using the Aperio Positive Pixel Count algorithm of the ImageScope analysis software (Leica Biosystems). The algorithm measured the intensity of each marker (red-pink/brown signal), and the percentage of weak and strong positive pixels was calculated relative to the total number of pixels in the section. Morphometric analysis was conducted on three consecutively cut lung sections from WT (n = 6 at 14, 21 and 28 days), Tie2PTX3 (n = 6 at 14, 21 and 28 days) and PTX3-KO (n = 4 at 14, 21 days; n = 0 at 28 days). Two independent observers (Ad'A and TA) randomly selected three layers *per* section *per* biopsy *per* mouse (1 mouse x 3 sections x 3 layers) at 40x magnification using the rectangle tools to determine the region of interest. All the layers were selected in the fibrotic lesions (results related to fibrosis were presented in the previous study [20]).

2.4. Statistical analysis

Six is the number of mice per experimental group except for PTX3-KO, which is four, because the homozygous absence of *Ptx3* in BLM-

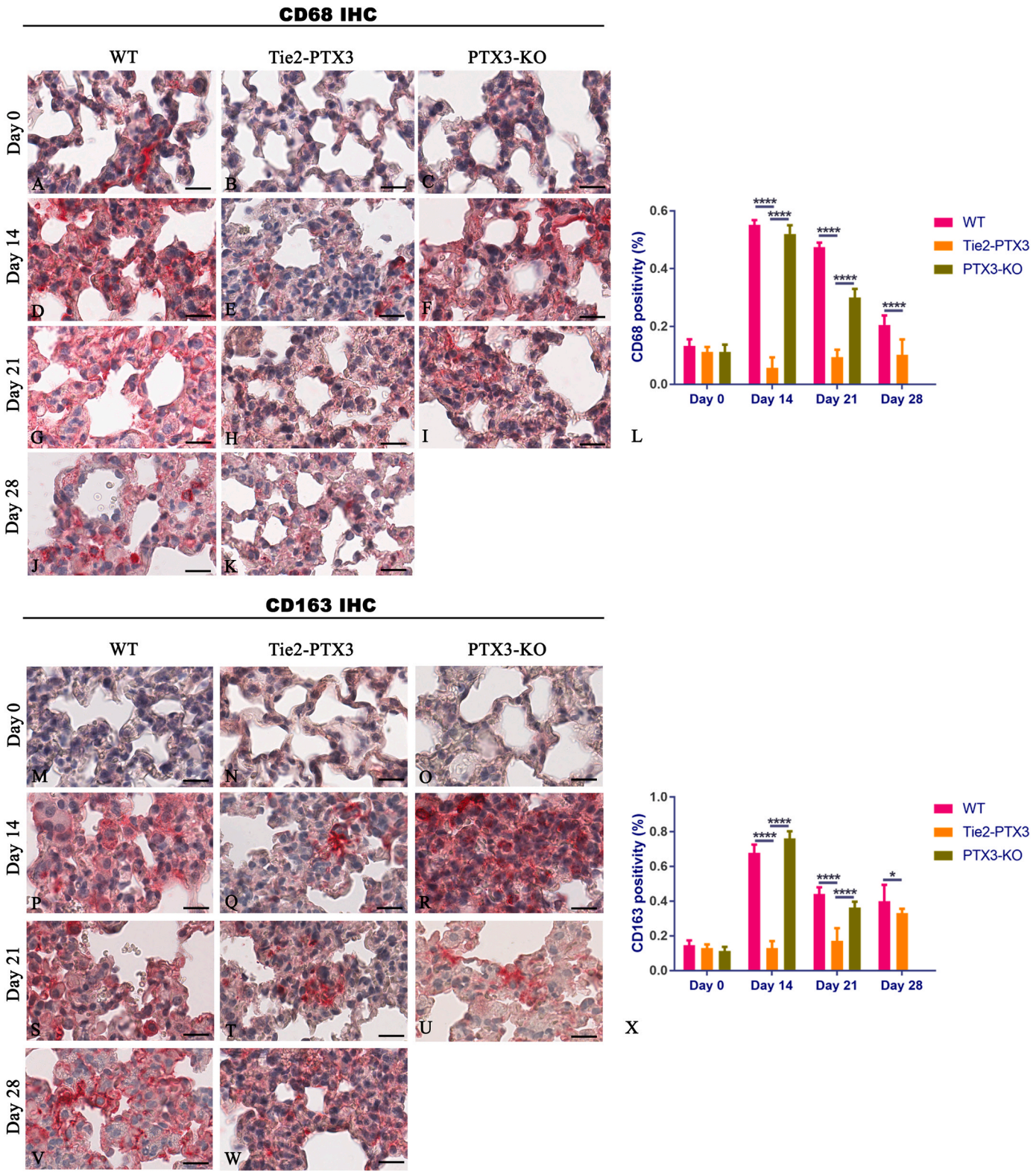

Fig. 1. PTX3 overexpression hampers CD68^{+} and anti-inflammatory CD163^{+} macrophage infiltration in BLM-induced lung fibrosis. CD68^{+} and CD163^{+} macrophages in the lungs of WT, Tie2-PTX3 and PTX3-KO mice, treated with BLM and sacrificed at different time points, were evaluated by immunohistochemistry and were estimated as a percentage on digital quantification within ROIs using the positive pixel count algorithm. Micrograph and immunostaining quantification show significantly fewer CD68^{+} and CD163^{+} macrophage infiltrate in mice overexpressing PTX3 (Tie2-PTX3; E, H, K for CD68 and; Q, T, W for CD163) compared with WT (D, G, J fro CD68; P, S, V for CD163) and PTX3-KO (F, I fro CD68; R, U for CD163) at different time points. No significant variations (L) were found in the same Tie2-PTX3 group (E, H, K) for CD68 at the different time points (Tie2-PTX3 at Day 14 (E) vs. Day 21 (H) vs. Day 28 (K)). For CD163, no significant variations (X) were found in Tie2-PTX3 on Day 14 (Q) vs. Day 21 (T), while it is on Day 21 (T) vs. Day 28 (W) ($p < 0.0001$). Data are reported as means ± SD, and the Tukey post-test was used to compare all groups after Two-way ANOVA. N = 6 mice for WT and Tie2PTX3 at 14, 21 and 28 days; N = 4 for PTX3-KO at 14 and 21 days; 6 or 4 mice x 3 sections each x 3 microscope layers each underwent morphometric analysis; Scale bar = 25 μm; *$p < 0.05$; * ** *$p < 0.0001$.

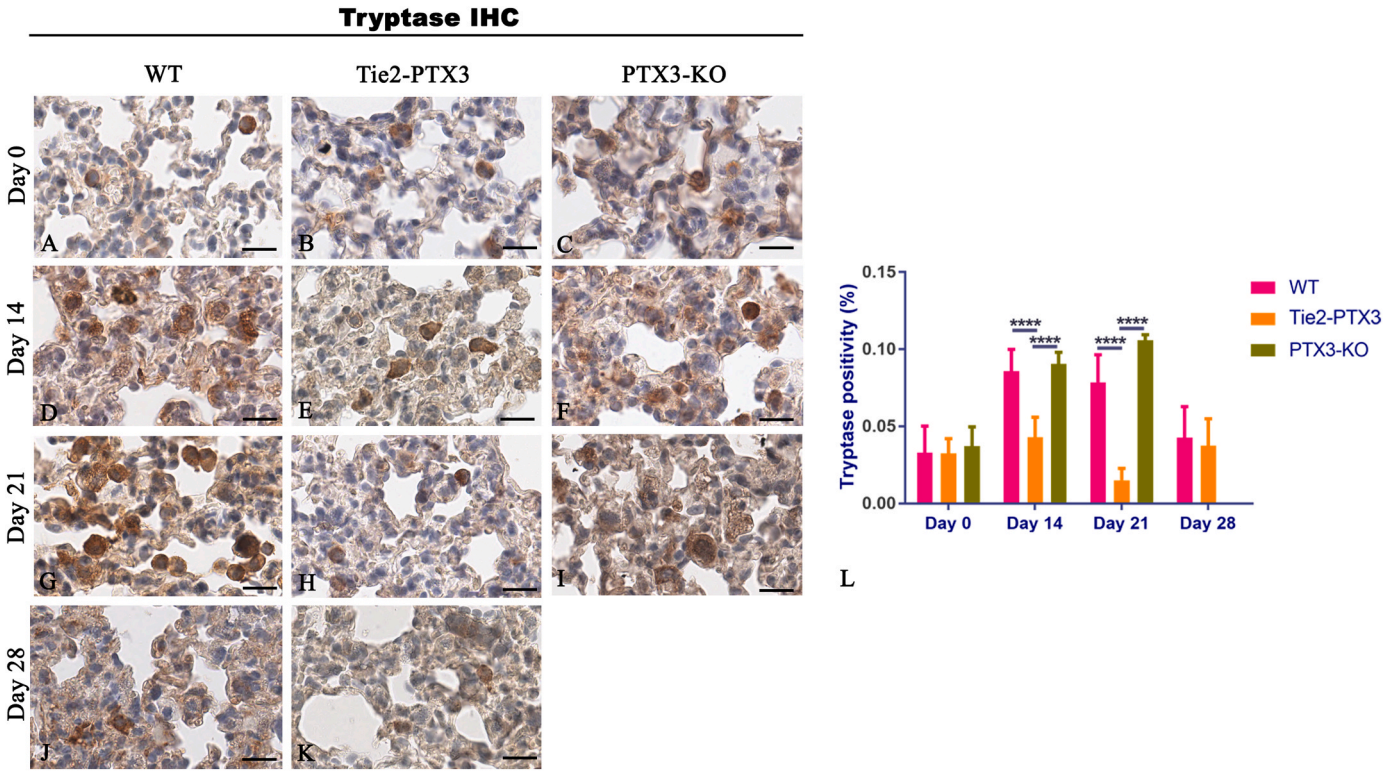

Fig. 2. PTX3 overexpression hampers Tryptase$^+$ mast cell infiltration in BLM-induced lung fibrosis. Tryptase$^+$ mast cells in the lungs of WT, Tie2-PTX3 and PTX3-KO mice, treated with BLM and sacrificed at different time points, were evaluated by immunohistochemistry and were estimated as a percentage on digital quantification within ROIs using the positive pixel count algorithm. Micrograph and immunostaining quantification show significantly fewer Tryptase$^+$ mast cell infiltrate in mice overexpressing PTX3 (Tie2-PTX3; E, H) compared with WT (D, G) and PTX3-KO (F, I) at the onset, Day 14 (D-F), and at the peak of fibrosis, Day 21 (G-I). Significant variations (L) were found in the same Tie2-PTX3 group on Day 14 (E) vs. Day 21 (H) ($p = 0.0048$), and on Day 21 (H) vs. Day 28 (K) ($p = 0.0323$). Data are reported as means ± SD, and the Tukey post-test was used to compare all groups after Two-way ANOVA. N = 6 mice for WT and Tie2PTX3 at 14, 21 and 28 days; N = 4 for PTX3-KO at 14 and 21 days; 6 or 4 mice x 3 sections each x 3 microscope layers each underwent morphometric analysis; Scale bar = 25 μm; * ** *$p < 0.0001$.

treated mice proved incompatible with life, and the PTX3-KO mice's mortality at day 28 was 100%.

Data graphs are presented as means ± SD (standard deviation). The distribution of datasets was assessed using a D'Agostino and Pearson omnibus normality test. Two-way ANOVA with post hoc Tukey's multiple comparisons test and Spearman nonparametric correlation analyses were performed using the GraphPad Prism software. P values less than 0.05 were considered significant and were summarized in Figure panels as * $p \leq 0.05$; ** $p \leq 0.01$; *** $p \leq 0.001$; **** $p \leq 0.0001$.

3. Results

In the present study, the immunostaining for the CD68 (Fig. 1), as a pan-macrophage marker, and CD163 (Fig. 1), as an M2-like macrophage marker, have shown a vast CD68$^+$ or CD163$^+$ cells in WT and PTX3-KO at all the time points investigated. In contrast, these macrophage populations were significantly less abundant in Tie2-PTX3 (Fig. 1) at all the time points analyzed, with no significant differences except that CD163 at day 21 vs. day 28 (Table 1).

In addition, lung fibrosis is sustained by mast cell protease Tryptase, which stimulates the proliferation of fibroblasts resident in the lung and induces collagen and fibronectin synthesis [46,47]. In our study, throughout the whole experimental period, the Tryptase$^+$ mast cells were detected in WT and PTX3-KO, while they were significantly less abundant in Tie2-PTX3 (Fig. 2) at all the time points investigated. A fluctuating trend was shown in Tie2-PTX3 with a down-expression on day 21 followed by an up-expression on day 28 at a level comparable to WT (Table 1).

T cells can have a profibrotic or antifibrotic role and distinct mechanisms to regulate fibrosis [48]. Looking at CD4$^+$ and CD8$^+$ T cells, we have found that their expression increases on day 14 compared with day 0 in all the experimental groups, but only for CD4$^+$ T cells in Tie2-PTX3 vs. WT and PTX3-KO there was a statistical significance (Fig. 3). On day 21, the PTX3 overexpression induced a reduction of both T cell subpopulations compared to WT and PTX3-KO (Fig. 3 H). On the contrary, in Tie2-PTX3, CD4$^+$ and CD8$^+$ infiltrates reincrease on day 28 (Fig. 3 K), while they appear reduced in WT (Fig. 3 J). This trend shows PTX3-mediated recruitment of T cells at the onset of fibrosis (day 14) and during partial regression (day 28) (Table 1). Therefore, PTX3 overexpression at the peak of fibrosis (day 21) strongly reduces T cell infiltrate (Fig. 3 H).

Because lung epithelial cells and fibroblasts play a crucial role in lung repair and regeneration, we have also evaluated the expression of the sex-determining region Y-box 2 (SOX2), a marker of conducting airways basal cells [49–51], and CD44, a marker of profibrogenic mesenchymal progenitor cells [52]. Our immunostaining for SOX2 (Fig. 4) showed significantly augmented SOX2$^+$ cells in WT and PTX3-KO on days 14 and 21 compared with days 0 and 28. In contrast, this staining was significantly reduced in Tie2-PTX3 (Fig. 4 E, H) at the same time points, with significant enhancement on day 21 vs. day 14 (Table 1).

For CD44, the micrographs and the morphological evaluation displayed slightly increased CD44$^+$ cells in Tie2-PTX3 (Fig. 5 E) compared to PTX3-KO on day 14, and an evident reduction in Tie2-PTX3 compared with WT (Fig. 5 G) and PTX3-KO (Fig. 5 I) at day 21 (Table 1).

Overall, our results demonstrated that PTX3 overexpression in the BLM-induced murine model of IPF carries out a protective role in: reducing CD68$^+$ and CD163$^+$ macrophage and the Tryptase$^+$ mast cell infiltrate in all phases of the disease; recruiting T cells at disease onset and during partial regression, while diminishing T cells infiltrate at

Table 1
Summary of the morphometric analysis performed following experimental groups.

Analysis	Days	EXPERIMENTAL GROUPS				
		WT	vs.	Tie2-PTX3	vs.	PTX3-KO
CD68 immunolabeling positivity	0	0.132777 ± 0.0227588	*ns*	0.1117087 ± 0.0177514	*ns*	0.1120454 ± 0.0250986
	14	0.5519618 ± 0.0163222	****	0.0574406 ± 0.0359285	* ** *	0.5201463 ± 0.0302643
	21	0.4753507 ± 0.0148447	* ** *	0.094429 ± 0.025476	* ** *	0.30039 ± 0.0299993
	28	0.2059916 ± 0.0323563	* ** *	0.1017171 ± 0.05361		
CD163 immunolabeling positivity	0	0.1464194 ± 0.0284938	*ns*	0.1294621 ± 0.0217523	*ns*	0.1138886 ± 0.0230739
	14	0.6786044 ± 0.0473531	* ** *	0.1300892 ± 0.0404032	* ** *	0.7619488 ± 0.0412854
	21	0.4420173 ± 0.038768	* ** *	0.1719378 ± 0.0726428	* ** *	0.3634561 ± 0.0332614
	28	0.400166 ± 0.094758	*	0.3313563 ± 0.0252598		
Tryptase immunolabeling positivity	0	0.033081 ± 0.017083	*ns*	0.0325731 ± 0.0094755	*ns*	0.0373217 ± 0.0123902
	14	0.0858034 ± 0.0141139	* ** *	0.0429984 ± 0.0129094	* ** *	0.0906 ± 0.007418
	21	0.078706 ± 0.017762	* ** *	0.0150047 ± 0.0078529	* ** *	0.1058497 ± 0.0036192
	28	0.04275669 ± 0.0200214	*ns*	0.0374736 ± 0.017502		
CD4 immunolabeling positivity	0	0.1063883 ± 0.08252259	*ns*	0.09359024 ± 0.03459115	*ns*	0.09561096 ± 0.02513327
	14	0.217349 ± 0.05736352	* ** *	0.594515 ± 0.07186317	* ** *	0.1442403 ± 0.0853022
	21	0.8434191 ± 0.1476787	* ** *	0.1015866 ± 0.08344486	* ** *	0.7012089 ± 0.2002902
	28	0.5504159 ± 0.07375775	*ns*	0.6765916 ± 0.07931086		
CD8 immunolabeling positivity	0	0.2359972 ± 0.0376369	ns	0.2757872 ± 0.0641826	ns	0.2019811 ± 0.0322504
	14	0.4285995 ± 0.0355274	ns	0.501625 ± 0.0365747	ns	0.4191636 ± 0.062666
	21	0.8675922 ± 0.1167428	* ** *	0.0988997 ± 0.0571437	* ** *	0.8268912 ± 0.0670832
	28	0.26617229 ± 0.0363403	ns	0.2960518 ± 0.0374027		
SOX2 immunolabeling positivity	0	0.2913101 ± 0.0423557	*ns*	0.3419417 ± 0.0250514	*ns*	0.259676 ± 0.0408797
	14	0.6601425 ± 0.0697052	* ** *	0.4093736 ± 0.070055	* ** *	0.7522773 ± 0.0543475
	21	0.9258334 ± 0.0949652	* ** *	0.7688214 ± 0.0415037	* ** *	0.961877 ± 0.0997067
	28	0.3685167 ± 0.0501708	*ns*	0.4060492 ± 0.024526		
CD44 immunolabeling positivity	0	0.4685167 ± 0.065273	*ns*	0.5227158 ± 0.0738974	*ns*	0.4830887 ± 0.064035
	14	0.6034759 ± 0.0675317	*ns*	0.5985847 ± 0.0290075	*	0.5043649 ± 0.0445696
	21	0.6551668 ± 0.0507363	* ** *	0.460311 ± 0.058906	* ** *	0.686877 ± 0.074675
	28	0.3079768 ± 0.0437652	* ** *	0.1579998 ± 0.0472571		

The morphometric values are expressed as mean ± SD (n = 6 for WT AND Tie2-PTX3; n = 4 for PTX3-KO) and have been utilized for the graphs in Fig. 1-7. Tukey's post-test was used to compare all groups after Two-way ANOVA and Spearman for correlation (ns, not significative; * $p \leq 0.05$; **** $p \leq 0.0001$).

disease peak; reducing SOX2 expression at disease onset and progression; reducing $CD44^+$ cells at disease peak (Table 2). Moreover, the statistical correlation has shown a positive and moderate correlation between CD44 and Tryptase and between SOX2 and CD8 expression (Fig. 6) by profibrogenic mesenchymal progenitor cells, mast cells, airway basal cells and T cells, respectively. At the same time, very strong and positive was the correlation between CD44 and CD8 expression by profibrogenic mesenchymal progenitor cells and T cells, respectively (Fig. 6).

4. Discussion

The novelty of this study was to investigate, in the BLM-induced murine model of IPF, the different effectors of immunity and tissue repair/regeneration events under the influence of PTX3 overexpression and deficiency in endothelial cells and stroma. We decided to select PTX3 overexpression in endothelial cells and stroma only, instead of the entire organism, in order to further investigate the role of endothelial cells in inflammatory processes. It is suggested that PTX3 produced by ECs and inflammatory cells may be affected by autocrine and paracrine ways, immune, lung epithelium and fibroblasts/myofibroblasts cells. For instance, PTX3 can bind various fibroblast growth factors (FGFs), inhibiting FGF-dependent angiogenesis [53] or FGF2-dependent smooth muscle cell proliferation, suppressing the mitogenic and chemotactic activity exerted on these cells [54].

Here, we have made a picture of the lung microenvironment of the BLM-induced pulmonary fibrosis mouse model by looking at macrophages, mast cells, and T cells during different stages of the disease. Moreover, we have looked at the transcription factor SOX2 and the adhesion-molecule promoting cell migration CD44, because they are involved in lung fibrosis after epithelial cell injury [49]. We took advantage of two transgenic mouse models, Tie2-PTX3 and PTX3-KO mice, to indirectly correlate the PTX3 expression effect to microenvironment cell composition.

In agreement with our data, in BLM-induced lung fibrosis mice, $CD163^+$ macrophages (M2-like) are reported to increase progressively, along with collagen deposition, until the maximum level on day 14 [55,56]. Based on the literature and our data, PTX3 constitutive overexpression could reduce macrophage recruitment/activation/repolarization in the Tie2-PTX3 experimental model. The reduced number of macrophages at fibroblastic foci and during all the disease progression under PTX3 overexpression could reduce the accumulation/release of profibrotic mediators, which stimulate fibroblast proliferation and collagen synthesis/deposition, by $CD163^+$ cells [57,58] in order to accelerate the resolution of inflammation. Future in-depth analyses are required to clarify whether PTX3 mediates these effects by blocking the recruitment, promoting apoptosis, or inhibiting the polarization of M2 macrophages or by a combination of these mechanisms. However, some studies demonstrated that PTX3 is involved in regulating macrophage activity. In fact, Shiraki et al. showed that PTX3 exposure significantly reduced macrophage IL-1β, TNF-α and MCP-1 levels, on the other hand increasing TGF− β levels. Moreover, PTX3 induced Akt phosphorylation and reduced nuclear factor-kappa B (NF-κB) activation in macrophages [59]. This evidence may explain the protective role exerted by PTX3 overexpression by reducing the levels of proinflammatory cytokines through specific intracellular pathways.

PTX3 overexpression shapes also mast cell infiltrate in the lung microenvironment. Based on our observations, we may assert that in the Tie2-PTX3 experimental model, PTX3 constitutive overexpression reduces $Tryptase^+$ mast cell recruitment/activation, which in turn reduces the activation/recruitment of $CD44^+$ myofibroblasts at fibroblastic foci as annotated by a pathologist [60]. Increased numbers of mast cells in pulmonary fibrosis [61] and clinical correlations between mast cells and fibrosis have been reported [62]. As demonstrated in prostate carcinoma, PTX3 may act by sequestering FGF2 and thereby blocking the capacity of mast cells to respond chemotattically to FGF2 [53].

It is now evident the role of T cells in fibrotic progression [63–69]. In lung biopsies of IPF patients, $CD8^+$ T cells are distributed more diffusely

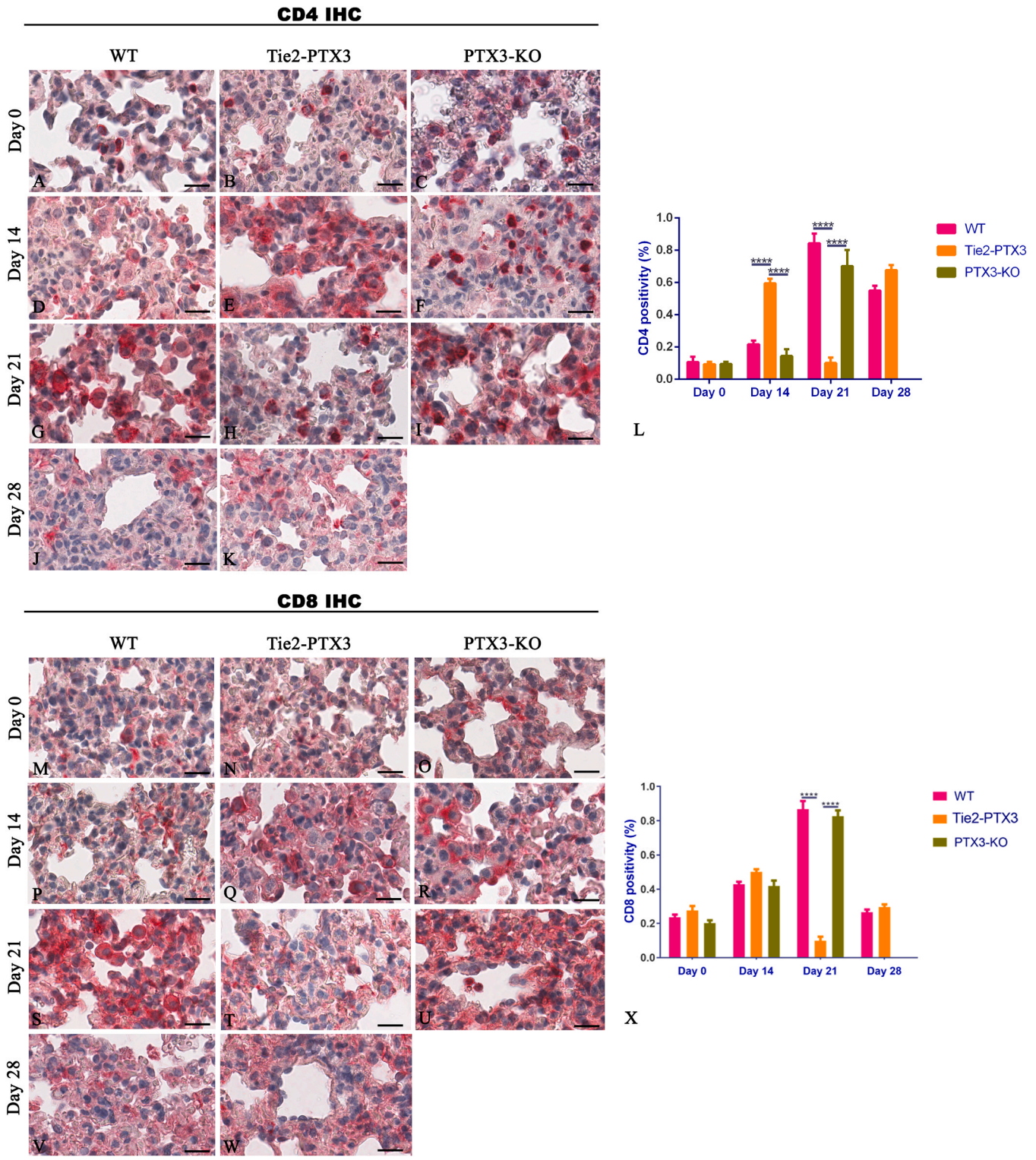

Fig. 3. PTX3 overexpression supports $CD4^+$ T cell infiltration in BLM-induced lung fibrosis at the onset and hampers $CD8^+$ T cell infiltration in BLM-induced lung fibrosis at the peak of fibrosis. $CD4^+$ and $CD8^+$ T cells in the lungs of WT, Tie2-PTX3 and PTX3-KO mice, treated with BLM and sacrificed at different time points, were evaluated by immunohistochemistry and were estimated as a percentage on digital quantification within ROIs using the positive pixel count algorithm. Micrograph and immunostaining quantification show a significantly higher $CD4^+$ T cells infiltrate in mice overexpressing PTX3 (Tie2-PTX3; E) compared with WT (D) and PTX3-KO (F) at Day 14, while it decreases at the peak of fibrosis, Day 21 (H), to reincreases later at partial fibrosis regression, Day 28 (K). For CD4, significant variations (L) were found in the same Tie2-PTX3 on Day 14 (E) vs. Day 21 (H) vs. Day 28 (K) ($p < 0.0001$). Micrograph and immunostaining quantification show significantly lower $CD8^+$ T cells infiltrate in mice overexpressing PTX3 (Tie2-PTX3; T) compared with WT (S) and PTX3-KO (U) at the peak of fibrosis, Day 21, while no significant differences are among all the experimental groups at Day 14 (P-R) and Day 28 (V, W).Data are reported as means ± SD, and the Tukey post-test was used to compare all groups after Two-way ANOVA. N = 6 mice for WT and Tie2PTX3 at 14, 21 and 28 days; N = 4 for PTX3-KO at 14 and 21 days; 6 or 4 mice x 3 sections each x 3 microscope layers each underwent morphometric analysis; Scale bar = 25 μm; * ** *$p < 0.0001$.

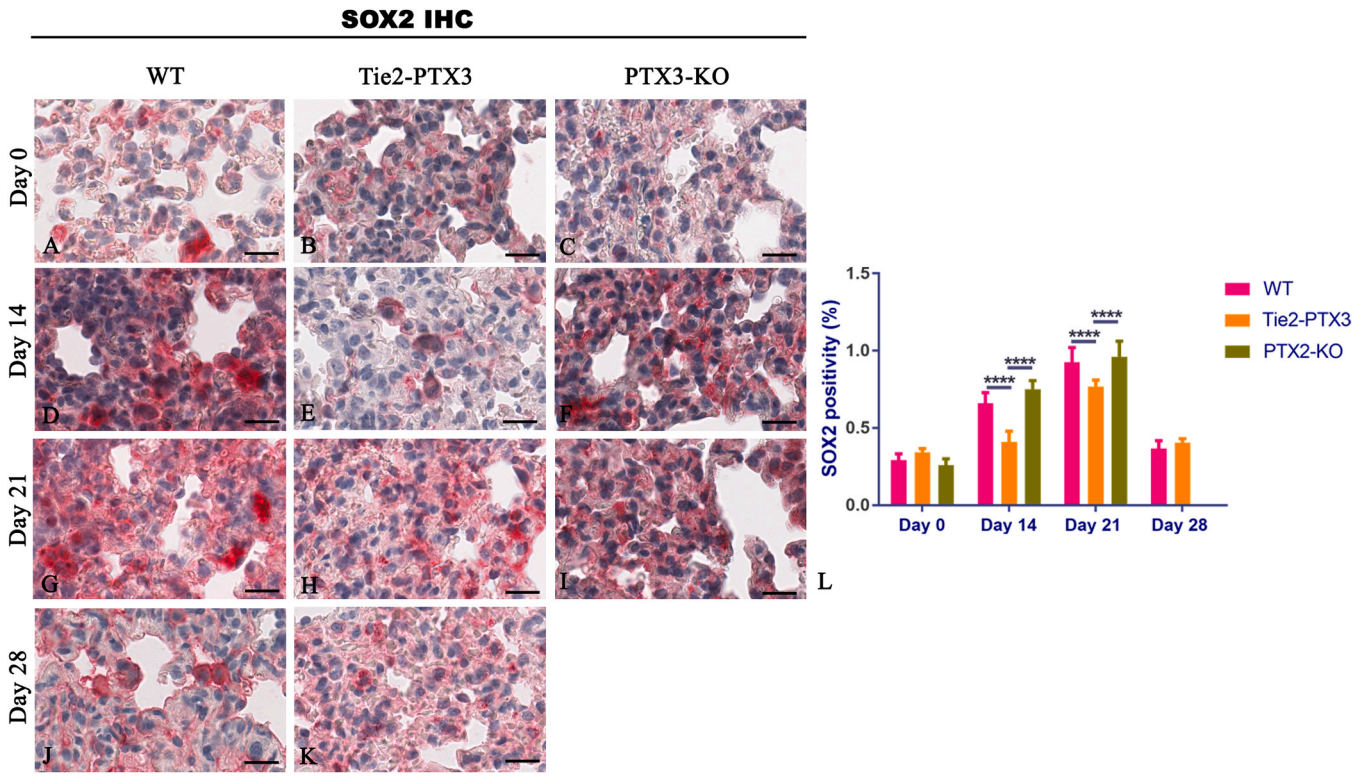

Fig. 4. PTX3 overexpression hampers the self-renewal associated transcription factor SOX2 expression in BLM-induced lung fibrosis. $SOX2^+$ stem cells in the lungs of WT, Tie2-PTX3 and PTX3-KO mice, treated with BLM and sacrificed at different time points, were evaluated by immunohistochemistry and were estimated as a percentage on digital quantification within ROIs using the positive pixel count algorithm. Micrograph and immunostaining quantification show significantly lower $SOX2^+$ stem cell extent in mice overexpressing PTX3 (Tie2-PTX3; E, H) compared with WT (D, G) and PTX3-KO (F, I) at the onset, Day 14 (D-F), and at the peak of fibrosis, Day 21 (G-I). Significant variations (L) were found in the same Tie2-PTX3 group on Day 14 (E) vs. Day 21 (H) ($p < 0.0001$), and on Day 21 (H) vs. Day 28 (K) ($p < 0.0001$). Data are reported as means ± SD, and the Tukey post-test was used to compare all groups after Two-way ANOVA. N = 6 mice for WT and Tie2PTX3 at 14, 21 and 28 days; N = 4 for PTX3-KO at 14 and 21 days; 6 or 4 mice x 3 sections each x 3 microscope layers each underwent morphometric analysis; Scale bar = 25 μm; * ** *$p < 0.0001$.

throughout the lung parenchyma and alveolar walls, associated with dyspnoea degree and functional parameters of disease severity [70]. In the BLM-induced pulmonary fibrosis model, $CD8^+$ T cells differentiate into profibrotic IL-13-producing Tc2 cells [70,71]. Furthermore, $CD8^+$ T cells in the fibrotic tissues of IPF can differentiate into cells that release IFN-γ but not IL-4, favorable for fibrosis reduction, and cells that produce IL-4 but not IFN-γ, stimulating fibrosis [72]. PTX3 inhibits the cross-presentation of apoptotic-cell-derived antigens to $CD8^+$ T cells [73], while its lack promotes autoimmune lung disease in a murine model of systemic lupus erythematosus [74]. In cutaneous Leishmaniasis, using a loss-of-function approach and in vitro experiments, it was demonstrated that PTX3 is a negative regulator of Th17, but does not affect Th1 polarization [75]. According to this crucial but controversial involvement of T cells in fibrotic progression and of PTX3 in regulating T cell, our results in Tie2-PTX3 experimental model demonstrated that PTX3 constitutive overexpression shapes $CD4^+$ and $CD8^+$ T cells recruitment/activation from disease onset to the regression phase but with a fluctuating trend probably due to a different activation of the different subtypes of T cell or to the release of different cytokines based on disease stage, lung parenchyma localization (epithelial cell or fibroblast/myofibroblast), or microenvironment (inflammatory or immunosuppressive) [76]. Further in-depth analyses concerning cytokines and generating polarized antigen-specific T cell effector populations will be necessary.

IPF has always been considered a fibroblast-driven disease. However, recent evidence demonstrated that it would be better to describe pathogenetically as an epithelium-driven disease in which dysfunctional, aging or microinjuried lung epithelial cells cannot sustain lung regeneration. The shift from regeneration to fibrosis results from the imbalance between profibrotic and antifibrotic pathways, which leads to chronic fibroblastic proliferation and collagen deposition [77]. In this more complex and better understood pathogenetic context, IPF may be a disease resulting from exhaustion of epithelial stem cells pool, consequently failing proper repair and instead leading to fibrotic scarring as pathological wound healing. Therefore, we studied the expression of SOX2, a marker of conducting airways basal cells [49–51], and CD44, a marker of pro-fibrogenic mesenchymal progenitor cells [52].

In agreement with the recent literature [50,78,79], that demonstrates a loss of normal regional proximal-peripheral cellular identity, leading to a loss of the normal proximal-peripheral differentiation of pulmonary epithelial cells and, as a consequence, to the disruption of alveolar structure, we observed a reduced amount of $SOX2^+$ epithelial cells and fibroblast-associated stem cells under PTX3 overexpression highlighting the protective role exerted by PTX3 and suggesting a possible beneficial effect in preventing cellular identity loss, alveolar structure disruption and fibrosis deposition. Moreover, in our study, the effects of PTX3 on reducing SOX2 expression seemed to be long-term. In fact, in Tie2-PTX3, we observed that SOX2 expression increases on day 21 compared to day 14, then decreases again. These data possibly suggest that chronic exposure to high levels of PTX3 may also overcome other pathways responsible for the alternative expression of SOX2 in lung epithelial cells, durably counteracting abnormal lung epithelial cell remodeling and alveolar disruption, also preventing fibroblast-associated stem cell acquisition and collagen synthesis in the lung.

The hyaluronic acid receptor CD44 is expressed by fibroblasts and epithelial cells in the lungs and is upregulated in radiation- and bleomycin-induced pulmonary fibrosis [57,80]. A recent study revealed

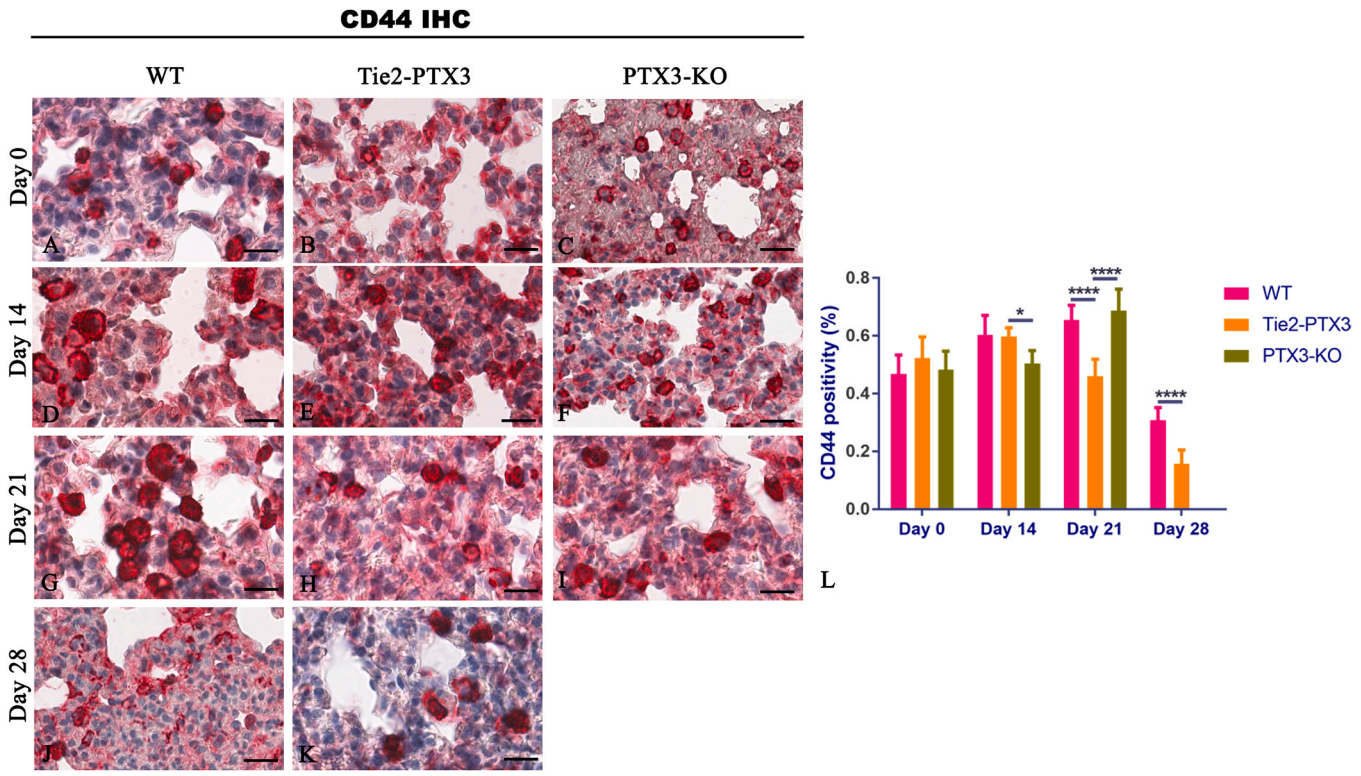

Fig. 5. PTX3 overexpression hampers the stem cell CD44 marker expression in BLM-induced lung fibrosis. $CD44^{+}$ stem cells in the lungs of WT, Tie2-PTX3 and PTX3-KO mice, treated with BLM and sacrificed at different time points, were evaluated by immunohistochemistry and were estimated as a percentage on digital quantification within ROIs using the positive pixel count algorithm. Micrograph and immunostaining quantification show a significantly lower $CD44^{+}$ stem cell extent in mice overexpressing PTX3 (Tie2-PTX3; E, H, K) compared with WT (G, J) and PTX3-KO (F, I) at the onset, Day 14 (E, F), and at the peak of fibrosis, Day 21 (G-I). Significant variations (L) were found in the same Tie2-PTX3 group on Day 14 (E) vs. Day 21 (H) ($p = 0.0004$), and on Day 21 (H) vs. Day 28 (K) ($p < 0.0001$). Data are reported as means ± SD, and the Tukey post-test was used to compare all groups after Two-way ANOVA. N = 6 mice for WT and Tie2PTX3 at 14, 21 and 28 days; N = 4 for PTX3-KO at 14 and 21 days; 6 or 4 mice x 3 sections each x 3 microscope layers each underwent morphometric analysis; Scale bar = 25 μm; *$p < 0.05$ * ; * ** *$p < 0.0001$.

that some mesenchymal progenitor cells (MPCs) show an increased CD44 expression and are the drivers of progressive fibrosis in IPF. CD44-high MPCs are present at the periphery of the IPF fibroblastic foci, in regions of active fibrogenesis, and have been demonstrated to be more fibrogenic than CD44-low IPF MPCs. Moreover, CD44 may accumulate within the nucleus as part of a nuclear protein complex that targets the SOX2 gene, promoting its upregulation [52]. CD44 is a PTX3 direct-binding receptor [81] and PTX3/CD44 pathway contributes to myofibroblast differentiation and lung fibrosis via PI3K-AKT1, NF-κB, and JNK intracellular signaling [82]. Therefore, based on the literature and our results, we may assert that PTX3 overexpression can reduce CD44 expression in MPCs during disease progression and not at disease onset, counteracting their differentiation into fibrogenic IPF MPCs and preventing uncontrolled and irreversible collagen deposition, which is responsible for the propagation of fibrosis and clinical progression of IPF. In fact, during the first phases of the disease, the main pathogenetic processes are epithelial injury and inflammatory infiltration, while fibrosis intervenes later and is a consequence of ineffective epithelial regeneration and repair.

5. Limitations of the study and its methodology

In this study, we build on a previous study to characterize the effects of PTX3 genetic overexpression and genetic depletion on the phenotypes of immune cells infiltrating the lung in the bleomycin injury model. The results demonstrated that PTX3 shapes profibrotic immune cells and epithelial/fibroblast repair and regeneration in a murine model of pulmonary fibrosis.

The main body of the presented data was derived using the immunohistochemical approach for characteristic markers of T cells, macrophages, mast cells, lung epithelium and fibroblasts/myofibroblasts. The whole-slide scanning Aperio platform was used at 40x magnification, and analyses were performed using the robust digital quantification Aperio Positive Pixel Count algorithm of the ImageScope analysis software [83,84]. The dataset presented in this study is voluminous, and the presentation of the findings is sufficiently systematic. The major strengths are the parallel use of wild-type, PTX-overexpressing and PTX3-deficient mice and the evaluation of the immunohistochemistry reactions by an expert pathologist. Despite the considerable amount of qualitative and quantitative data presented, the comparison across these three groups of animals allows for mechanistic conclusions and presents some limitations.

While robust digital quantification exists, this relies solely on a single biomarker to determine cell types and, therefore, can lead to inaccuracies. Single-cell sequencing, flow cytometry, additional cell-specific markers, or other detailed quantitative experimental approaches could have more robustly confirmed the results. However, several studies use immunohistochemical evaluation as a sufficient rationale (e.g. for CD4 and CD8 are employed to conclude about T cell numbers [85,86]), and this histopathological approach gives information about the type of cells present and further information regarding the localization of these cells and the relationship with other surrounding cells.

Concerning the mouse model, histologically, the changes in the lungs in the bleomycin model are quite different from the lungs of patients with IPF [87], as is the entire course of the disease. This model is still informative and valuable, but the conclusions should not be expanded to human disease without direct experimental confirmation.

Table 2
Summary of the morphometric analysis performed following experimental time.

Analysis	Experimental group	EXPERIMENTAL TIME						
		Day 0	vs.	Day 14	vs.	Day 21	vs.	Day 28
CD68 immunolabeling positivity	**WT**	0.132777 ± 0.0227588	* ** *	0.5519618 ± 0.0163222	* **	0.4753507 ± 0.0148447	* ** *	0.2059916 ± 0.0323563
	Tie2-PTX3	0.111708 ± 0.0177514	*	0.0574406 ± 0.0359285	ns	0.094429 ± 0.025476	ns	0.1017171 ± 0.05361
	PTX3-KO	0.112045 ± 0.0250986	* ** *	0.5201463 ± 0.0302643	* ** *	0.30039 ± 0.0299993	* ** *	
CD163 immunolabeling positivity	**WT**	0.1464194 ± 0.0284938	* ** *	0.6786044 ± 0.0473531	* ** *	0.4420173 ± 0.038768	ns	0.400166 ± 0.094758
	Tie2-PTX3	0.1294621 ± 0.0217523	*ns*	0.1300892 ± 0.0404032	ns	0.1719378 ± 0.0726428	* ** *	0.3313563 ± 0.0252598
	PTX3-KO	0.1138886 ± 0.0230739	* ** *	0.7619488 ± 0.0412854	* ** *	0.3634561 ± 0.0332614	* ** *	
Tryptase immunolabeling positivity	**WT**	0.033081 ± 0.017083	* ** *	0.0858034 ± 0.0141139	ns	0.078706 ± 0.017762	* **	0.04275669 ± 0.0200214
	Tie2-PTX3	0.0325731 ± 0.0094755	*ns*	0.0429984 ± 0.0129094	* *	0.0150047 ± 0.0078529	*	0.0374736 ± 0.017502
	PTX3-KO	0.0373217 ± 0.0123902	* ** *	0.0906 ± 0.007418	ns	0.1058497 ± 0.0036192	* ** *	
CD4immunolabeling positivity	**WT**	0.1063883 ± 0.08252259	*ns*	0.217349 ± 0.05736352	* ** *	0.8434191 ± 0.1476787	* ** *	0.5504159 ± 0.07375775
	Tie2-PTX3	0.09359024 ± 0.03459115	* ** *	0.594515 ± 0.07186317	* ** *	0.1015866 ± 0.08344486	* ** *	0.6765916 ± 0.07931086
	PTX3-KO	0.09561096 ± 0.02513327	*ns*	0.1442403 ± 0.0853022	* ** *	0.7012089 ± 0.2002902	* ** *	
CD8 immunolabeling positivity	**WT**	0.2359972 ± 0.0376369	* ** *	0.4285995 ± 0.0355274	* ** *	0.8675922 ± 0.1167428	* ** *	0.26617229 ± 0.0363403
	Tie2-PTX3	0.2757872 ± 0.0641826	* ** *	0.501625 ± 0.0365747	* ** *	0.0988997 ± 0.0571437	* ** *	0.2960518 ± 0.0374027
	PTX3-KO	0.2019811 ± 0.0322504	* ** *	0.4191636 ± 0.062666	* ** *	0.8268912 ± 0.0670832	* ** *	
SOX2 immunolabeling positivity	**WT**	0.2913101 ± 0.0423557	* ** *	0.6601425 ± 0.0697052	* ** *	0.9258334 ± 0.0949652	* ** *	0.3685167 ± 0.0501708
	Tie2-PTX3	0.3419417 ± 0.0250514	*ns*	0.4093736 ± 0.070055	* ** *	0.7688214 ± 0.0415037	* ** *	0.4060492 ± 0.024526
	PTX3-KO	0.259676 ± 0.0408797	* ** *	0.7522773 ± 0.0543475	* ** *	0.961877 ± 0.0997067	* ** *	
CD44 immunolabeling positivity	**WT**	0.4685167 ± 0.065273	* **	0.6034759 ± 0.0675317	*ns*	0.6551668 ± 0.0507363	* ** *	0.3079768 ± 0.0437652
	Tie2-PTX3	0.5227158 ± 0.0738974	*ns*	0.5985847 ± 0.0290075	* **	0.460311 ± 0.058906	* ** *	0.1579998 ± 0.0472571
	PTX3-KO	0.4830887 ± 0.064035	*ns*	0.5043649 ± 0.0445696	* **	0.686877 ± 0.074675	* ** *	

The morphometric values are expressed as mean ± SD (n = 6 for WT AND Tie2-PTX3; n = 4 for PTX3-KO) and have been utilized for the graphs in Fig. 1-7. Tukey's post-test was used to compare all groups after Two-way ANOVA and Spearman for correlation (ns, not significative; * $p \leq 0.05$; **$p \leq 0.01$; ***$p \leq 0.001$; **** $p \leq 0.0001$).

6. Conclusions

Clinical management of IPF remains a major challenge in the absence of validated diagnostic tools and disease progression/activity criteria [88]. Furthermore, IPF has few therapeutic options, and lung transplantation represents the only curative option currently available, with an elevated risk of recurrence. Treatments that can stop or reverse the lungs' scarring are surely needed to prevent disrupted epithelial regeneration and consequent progressive and irreversible collagen deposition. Therefore, a better understanding of IPF pathogenic mechanisms, particularly of the complex microenvironment of the lung, is essential to identify new therapeutic targets and surrogate markers that could serve diagnostic purposes. Our observational results of the effect of PTX3 overexpression and deficiency on the pulmonary microenvironment at 14 (disease onset), 21 (disease peak) and 28 (disease regression) days of disease corroborate the protective role of PTX3 and lays the foundations for the deepening of the mechanisms of action of PTX3 on cellular and non-cellular components of the pulmonary microenvironment in BLM-treated mice. The role of PTX3 on profibrotic immune cells and epithelial/fibroblast repair and regeneration actors in a murine model of pulmonary fibrosis might represent a model to understand better the pro-immune and -fibrogenic microenvironment involved in the coordination of the cross-talks among MPCs, fibroblasts, macrophages, mast cells and T cells in order to prevent fibrosis in BLM-treated mice. Further studies will be necessary to translate these results into humans and better understand how PTX3 acts on microenvironment cells during lung fibrosis (for example, which cell signaling mechanisms are activated or suppressed?).

Ethics approval

The study was conducted on archival material belonging to the project approved with authorization 118/2017 reviewed and approved by Organismo Preposto al Benessere degli Animali (OPBA) University of Brescia.

Funding

This research received no external funding.

CRediT authorship contribution statement

Conceptualization, **R. Ronca**, **D. Ribatti**, and **T. Annese**; Methodology, **F. Maccarinnelli**, **M. Turati**, **L. Lorusso** and **M. De Giorgis**;

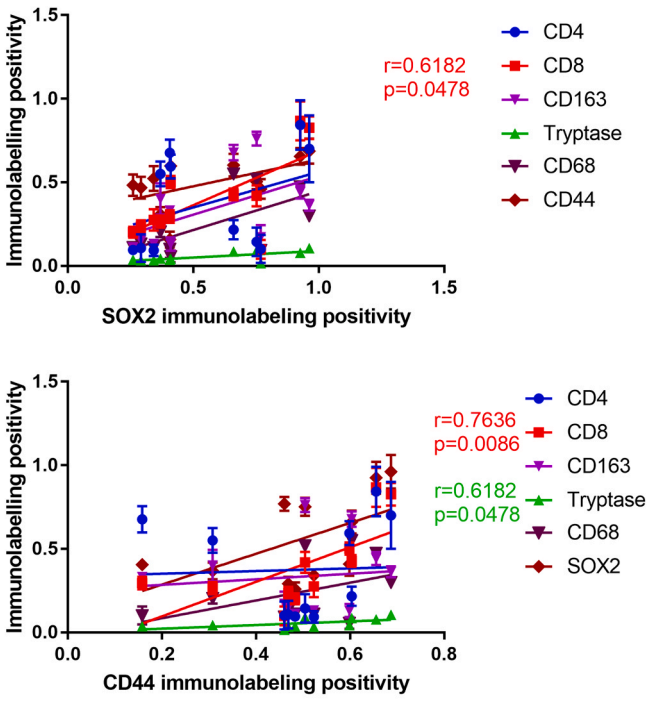

Fig. 6. Linear regression analysis (A) shows a positive and very strong statistical correlation between the CD44 and CD8 expression and a moderate one between CD44 and Tryptase. [For CD8: Y= 1034 *X - 0,11039; For Tryptase: Y = 0,1089 *X + 0,0008092]. Linear regression analysis (B) shows a positive and very strong statistical correlation between the SOX2 and CD8 expression. [For CD8: Y = 0,6529 *X + 0,03693].

Software, **R. Tmma**; Validation, **A. d'Amati** and **T. Annese**; Formal analysis, **F. Maccarinelli**, **M. Turati**, **L. Lorusso** and **A. d'Amati**; Investigation, **A. d'Amati** and **T. Annese**; Resources, R. Ronca and **D. Ribatti**; Data curation, **A. d'Amati** and **T. Annese**; Writing – original draft, **A. d'Amati** and **T. Annese**; Writing – review & editing, **D. Ribatti** and **T. Annese**; Visualization, T. **Annese**; Supervision, **T. Annese**. All authors have read and agreed to the published version of the manuscript.

Declaration of Competing Interest

All the authors have no declaration of interest statement.

References

[1] R. Krishna, K. Chapman, S. Ullah, Idiopathic pulmonary fibrosis. StatPearls, Treasure Isl. (2022).

[2] D.J. Lederer, F.J. Martinez, Idiopathic pulmonary fibrosis, N. Engl. J. Med. 378 (2018) 1811–1823, https://doi.org/10.1056/NEJMra1705751.

[3] W. Bae, C.H. Lee, J. Lee, Y.W. Kim, K. Han, S.M. Choi, Impact of smoking on the development of idiopathic pulmonary fibrosis: results from a nationwide population-based cohort study, Thorax 77 (2022) 470–476, https://doi.org/10.1136/thoraxjnl-2020-215386.

[4] V. Bellou, L. Belbasis, E. Evangelou, Tobacco smoking and risk for pulmonary fibrosis: a prospective cohort study from the UK biobank, Chest 160 (2021) 983–993, https://doi.org/10.1016/j.chest.2021.04.035.

[5] G. Paolocci, I. Folletti, K. Toren, M. Ekstrom, M. Dell'Omo, G. Muzi, N. Murgia, Occupational risk factors for idiopathic pulmonary fibrosis in Southern Europe: a case-control study, BMC Pulm. Med. 18 (2018), 75, https://doi.org/10.1186/s12890-018-0644-2.

[6] M. Ricco, Lung fibrosis and exposure to wood dusts: two case reports and review of the literature, Med Pr. 66 (2015) 739–747, https://doi.org/10.13075/mp.5893.00140.

[7] N.J. Awadalla, A. Hegazy, R.A. Elmetwally, I. Wahby, Occupational and environmental risk factors for idiopathic pulmonary fibrosis in Egypt: a multicenter case-control study, Int. J. Occup. Environ. Med. 3 (2012) 107–116.

[8] M. Baqir, A. Vasirreddy, A.N. Vu, T. Moua, A.M. Chamberlain, R.D. Frank, J. H. Ryu, Idiopathic pulmonary fibrosis and gastroesophageal reflux disease: a population-based, case-control study, Respir. Med. 178 (2021), 106309, https://doi.org/10.1016/j.rmed.2021.106309.

[9] H. Wang, Y. Zhuang, H. Peng, M. Cao, Y. Li, Q. Xu, X. Xin, K. Zhou, G. Liang, H. Cai, J. Dai, The relationship between MUC5B promoter, TERT polymorphisms and telomere lengths with radiographic extent and survival in a Chinese IPF cohort, Sci. Rep. 9 (2019), 15307, https://doi.org/10.1038/s41598-019-51902-6.

[10] D. Zhang, G. Povysil, P.H. Kobeissy, Q. Li, B. Wang, M. Amelotte, H. Jaouadi, C. A. Newton, T.M. Maher, P.L. Molyneaux, I. Noth, F.J. Martinez, G. Raghu, J. L. Todd, S.M. Palmer, C. Haefliger, A. Platt, S. Petrovski, J.A. Garcia, D. B. Goldstein, C.K. Garcia, Rare and common variants in KIF15 contribute to genetic risk of idiopathic pulmonary fibrosis, Am. J. Respir. Crit. Care Med. (2022), https://doi.org/10.1164/rccm.202110-2439OC.

[11] F.J. Martinez, H.R. Collard, A. Pardo, G. Raghu, L. Richeldi, M. Selman, J. J. Swigris, H. Taniguchi, A.U. Wells, Idiopathic pulmonary fibrosis, Nat. Rev. Dis. Prim. 3 (2017), 17074, https://doi.org/10.1038/nrdp.2017.74.

[12] S.L.F. Walsh, L. Calandriello, M. Silva, N. Sverzellati, Deep learning for classifying fibrotic lung disease on high-resolution computed tomography: a case-cohort study, Lancet Respir. Med. 6 (2018) 837–845, https://doi.org/10.1016/S2213-2600(18)30286-8.

[13] L.M. Glenn, T.J. Corte, Diagnosing idiopathic pulmonary fibrosis: has the time for surgical lung biopsy passed? Respirology 25 (2020) 1112–1113, https://doi.org/10.1111/resp.13909.

[14] M.J. van Manen, J.J. Geelhoed, N.C. Tak, M.S. Wijsenbeek, Optimizing quality of life in patients with idiopathic pulmonary fibrosis, Ther. Adv. Respir. Dis. 11 (2017) 157–169, https://doi.org/10.1177/1753465816686743.

[15] K. Borensztajn, B. Crestani, M. Kolb, Idiopathic pulmonary fibrosis: from epithelial injury to biomarkers–insights from the bench side, Respiration 86 (2013) 441–452, https://doi.org/10.1159/000357598.

[16] T.E. King Jr., A. Pardo, M. Selman, Idiopathic pulmonary fibrosis, Lancet 378 (2011) 1949–1961, https://doi.org/10.1016/S0140-6736(11)60052-4.

[17] N. Idiopathic Pulmonary Fibrosis Clinical Research, G. Raghu, K.J. Anstrom, T. E. King Jr., J.A. Lasky, F.J. Martinez, Prednisone, azathioprine, and N-acetylcysteine for pulmonary fibrosis, N. Engl. J. Med. 366 (2012) 1968–1977, https://doi.org/10.1056/NEJMoa1113354.

[18] A.A. van Batenburg, M.F.M. van Oosterhout, S.N. Knoppert, K.M. Kazemier, J. J. van der Vis, J.C. Grutters, R. Goldschmeding, C.H.M. van Moorsel, The extent of inflammatory cell infiltrate and fibrosis in lungs of telomere- and surfactant-related familial pulmonary fibrosis, Front. Med. 8 (2021), 736485, https://doi.org/10.3389/fmed.2021.736485.

[19] E. Balestro, F. Calabrese, G. Turato, F. Lunardi, E. Bazzan, G. Marulli, D. Biondini, E. Rossi, A. Sanduzzi, F. Rea, C. Rigobello, D. Gregori, S. Baraldo, P. Spagnolo, M. G. Cosio, M. Saetta, Immune inflammation and disease progression in idiopathic pulmonary fibrosis, PLoS One 11 (2016), e0154516, https://doi.org/10.1371/journal.pone.0154516.

[20] F. Maccarinelli, M. Bugatti, A. Churruca Schuind, S. Ganzerla, W. Vermi, M. Presta, R. Ronca, Endogenous long pentraxin 3 exerts a protective role in a murine model of pulmonary fibrosis, Front Immunol. 12 (2021), 617671, https://doi.org/10.3389/fimmu.2021.617671.

[21] A. Doni, M. Stravalaci, A. Inforzato, E. Magrini, A. Mantovani, C. Garlanda, B. Bottazzi, The long pentraxin PTX3 as a link between innate immunity, tissue remodeling, and cancer, Front Immunol. 10 (2019), 712, https://doi.org/10.3389/fimmu.2019.00712.

[22] J. Zhang, G. Zhao, J. Lin, C. Che, C. Li, N. Jiang, L. Hu, Q. Wang, Role of PTX3 in corneal epithelial innate immunity against Aspergillus fumigatus infection, Exp. Eye Res. 167 (2018) 152–162, https://doi.org/10.1016/j.exer.2016.11.017.

[23] F. Moalli, M. Paroni, T. Veliz Rodriguez, F. Riva, N. Polentarutti, B. Bottazzi, S. Valentino, S. Mantero, M. Nebuloni, A. Mantovani, A. Bragonzi, C. Garlanda, The therapeutic potential of the humoral pattern recognition molecule PTX3 in chronic lung infection caused by Pseudomonas aeruginosa, J. Immunol. 186 (2011) 5425–5434, https://doi.org/10.4049/jimmunol.1002035.

[24] G.Q. Shi, L. Yang, L.Y. Shan, L.Z. Yin, W. Jiang, H.T. Tian, D.D. Yang, Investigation of the clinical significance of detecting PTX3 for community-acquired pneumonia, Eur. Rev. Med. Pharm. Sci. 24 (2020) 8477–8482, https://doi.org/10.26355/eurrev_202008_22645.

[25] P.C. Reading, S. Bozza, B. Gilbertson, M. Tate, S. Moretti, E.R. Job, E.C. Crouch, A. G. Brooks, L.E. Brown, B. Bottazzi, L. Romani, A. Mantovani, Antiviral activity of the long chain pentraxin PTX3 against influenza viruses, J. Immunol. 180 (2008) 3391–3398, https://doi.org/10.4049/jimmunol.180.5.3391.

[26] R. Porte, S. Davoudian, F. Asgari, R. Parente, A. Mantovani, C. Garlanda, B. Bottazzi, The long pentraxin PTX3 as a humoral innate immunity functional player and biomarker of infections and sepsis, Front Immunol. 10 (2019), 794, https://doi.org/10.3389/fimmu.2019.00794.

[27] J. Balhara, L. Koussih, J. Zhang, A.S. Gounni, Pentraxin 3: an immuno-regulator in the lungs, Front Immunol. 4 (2013) 127, https://doi.org/10.3389/fimmu.2013.00127.

[28] S.N. Diniz, R. Nomizo, P.S. Cisalpino, M.M. Teixeira, G.D. Brown, A. Mantovani, S. Gordon, L.F. Reis, A.A. Dias, PTX3 function as an opsonin for the dectin-1-dependent internalization of zymosan by macrophages, J. Leukoc. Biol. 75 (2004) 649–656, https://doi.org/10.1189/jlb.0803371.

[29] M. Erreni, A.A. Manfredi, C. Garlanda, A. Mantovani, P. Rovere-Querini, The long pentraxin PTX3: A prototypical sensor of tissue injury and a regulator of homeostasis, Immunol. Rev. 280 (2017) 112–125, https://doi.org/10.1111/imr.12570.

[30] A. Doni, C. Garlanda, B. Bottazzi, S. Meri, P. Garred, A. Mantovani, Interactions of the humoral pattern recognition molecule PTX3 with the complement system,

Immunobiology 217 (2012) 1122–1128, https://doi.org/10.1016/j.imbio.2012.07.004.
[31] A. Doni, C. Garlanda, A. Mantovani, PTX3 orchestrates tissue repair, Oncotarget 6 (2015) 30435–30436, https://doi.org/10.18632/oncotarget.5453.
[32] C. Garlanda, B. Bottazzi, E. Magrini, A. Inforzato, A. Mantovani, PTX3, a humoral pattern recognition molecule, in innate immunity, tissue repair, and cancer, Physiol. Rev. 98 (2018) 623–639, https://doi.org/10.1152/physrev.00016.2017.
[33] A. Doni, T. Musso, D. Morone, A. Bastone, V. Zambelli, M. Sironi, C. Castagnoli, I. Cambieri, M. Stravalaci, F. Pasqualini, I. Laface, S. Valentino, S. Tartari, A. Ponzetta, V. Maina, S.S. Barbieri, E. Tremoli, A.L. Catapano, G.D. Norata, B. Bottazzi, C. Garlanda, A. Mantovani, An acidic microenvironment sets the humoral pattern recognition molecule PTX3 in a tissue repair mode, J. Exp. Med. 212 (2015) 905–925, https://doi.org/10.1084/jem.20141268.
[34] E. Magrini, A. Mantovani, C. Garlanda, The dual complexity of PTX3 in health and disease: a balancing act? Trends Mol. Med. 22 (2016) 497–510, https://doi.org/10.1016/j.molmed.2016.04.007.
[35] T. Mauri, V. Zambelli, C. Cappuzzello, G. Bellani, E. Dander, M. Sironi, V. Castiglioni, A. Doni, A. Mantovani, A. Biondi, C. Garlanda, G. D'Amico, A. Pesenti, Intraperitoneal adoptive transfer of mesenchymal stem cells enhances recovery from acid aspiration acute lung injury in mice, Intensive Care Med. Exp. 5 (2017), 13, https://doi.org/10.1186/s40635-017-0126-5.
[36] M. Yoshida, H. Oishi, T. Martinu, D.M. Hwang, H. Takizawa, J. Sugihara, T. D. McKee, X. Bai, Z. Guana, C. Lua, H.R. Cho, S. Juvet, M. Cypel, S. Keshavjee, M. Liu, Pentraxin 3 deficiency enhances features of chronic rejection in a mouse orthotopic lung transplantation model, Oncotarget 9 (2018) 8489–8501, https://doi.org/10.18632/oncotarget.23902.
[37] S. Kasuda, R. Kudo, K. Yuui, Y. Sakurai, K. Hatake, Acute ethanol intoxication suppresses pentraxin 3 expression in a mouse sepsis model involving cecal ligation and puncture, Alcohol 64 (2017) 1–9, https://doi.org/10.1016/j.alcohol.2017.04.003.
[38] S. Jaillon, G. Mancuso, Y. Hamon, C. Beauvillain, V. Cotici, A. Midiri, B. Bottazzi, M. Nebuloni, C. Garlanda, I. Fremaux, J.F. Gauchat, P. Descamps, C. Beninati, A. Mantovani, P. Jeannin, Y. Delneste, Prototypic long pentraxin PTX3 is present in breast milk, spreads in tissues, and protects neonate mice from Pseudomonas aeruginosa lung infection, J. Immunol. 191 (2013) 1873–1882, https://doi.org/10.4049/jimmunol.1201642.
[39] R.G. Jenkins, B.B. Moore, R.C. Chambers, O. Eickelberg, M. Konigshoff, M. Kolb, G. J. Laurent, C.B. Nanthakumar, M.A. Olman, A. Pardo, M. Selman, D. Sheppard, P. J. Sime, A.M. Tager, A.L. Tatler, V.J. Thannickal, E.S. White, A.T.S.Ao.R. Cell, B. Molecular, An Official American Thoracic Society Workshop Report: use of animal models for the preclinical assessment of potential therapies for pulmonary fibrosis, Am. J. Respir. Cell Mol. Biol. 56 (2017) 667–679, https://doi.org/10.1165/rcmb.2017-0096ST.
[40] J. Tashiro, G.A. Rubio, A.H. Limper, K. Williams, S.J. Elliot, I. Ninou, V. Aidinis, A. Tzouvelekis, M.K. Glassberg, Exploring animal models that resemble idiopathic pulmonary fibrosis, Front. Med. 4 (2017), 118, https://doi.org/10.3389/fmed.2017.00118.
[41] D. Pilling, N. Cox, V. Vakil, J.S. Verbeek, R.H. Gomer, The long pentraxin PTX3 promotes fibrocyte differentiation, PLoS One 10 (2015), e0119709, https://doi.org/10.1371/journal.pone.0119709.
[42] R.C. Russo, B. Savino, M. Mirolo, C. Buracchi, G. Germano, A. Anselmo, L. Zammataro, F. Pasqualini, A. Mantovani, M. Locati, M.M. Teixeira, The atypical chemokine receptor ACKR2 drives pulmonary fibrosis by tuning influx of CCR2(+) and CCR5(+) IFNgamma-producing gammadeltaT cells in mice, Am. J. Physiol. Lung Cell Mol. Physiol. 314 (2018) L1010–L1025, https://doi.org/10.1152/ajplung.00233.2017.
[43] C. Garlanda, E. Hirsch, S. Bozza, A. Salustri, M. De Acetis, R. Nota, A. Maccagno, F. Riva, B. Bottazzi, G. Peri, A. Doni, L. Vago, M. Botto, R. De Santis, P. Carminati, G. Siracusa, F. Altruda, A. Vecchi, L. Romani, A. Mantovani, Non-redundant role of the long pentraxin PTX3 in anti-fungal innate immune response, Nature 420 (2002) 182–186, https://doi.org/10.1038/nature01195.
[44] R. Ronca, A. Giacomini, E. Di Salle, D. Coltrini, K. Pagano, L. Ragona, S. Matarazzo, S. Rezzola, D. Maiolo, R. Torrella, E. Moroni, R. Mazzieri, G. Escobar, M. Mor, G. Colombo, M. Presta, Long-pentraxin 3 derivative as a small-molecule FGF trap for cancer therapy, Cancer Cell 28 (2015) 225–239, https://doi.org/10.1016/j.ccell.2015.07.002.
[45] T. Annese, R. Ronca, R. Tamma, A. Giacomini, S. Ruggieri, E. Grillo, M. Presta, D. Ribatti, PTX3 modulates neovascularization and immune inflammatory infiltrate in a murine model of fibrosarcoma, Int J. Mol. Sci. 20 (2019), https://doi.org/10.3390/ijms20184599.
[46] I.A. Akers, M. Parsons, M.R. Hill, M.D. Hollenberg, S. Sanjar, G.J. Laurent, R. J. McAnulty, Mast cell tryptase stimulates human lung fibroblast proliferation via protease-activated receptor-2, Am. J. Physiol. Lung Cell Mol. Physiol. 278 (2000) L193–L201, https://doi.org/10.1152/ajplung.2000.278.1.L193.
[47] M. Wygrecka, G. Kwapiszewska, E. Jablonska, S. von Gerlach, I. Henneke, D. Zakrzewicz, A. Guenther, K.T. Preissner, P. Markart, Role of protease-activated receptor-2 in idiopathic pulmonary fibrosis, Am. J. Respir. Crit. Care Med. 183 (2011) 1703–1714, https://doi.org/10.1164/rccm.201009-1479OC.
[48] M. Zhang, S. Zhang, T cells in fibrosis and fibrotic diseases, Front. Immunol. 11 (2020), 1142, https://doi.org/10.3389/fimmu.2020.01142.
[49] E. Eenjes, D. Tibboel, R.M.H. Wijnen, J.M. Schnater, R.J. Rottier, SOX2 and SOX21 in lung epithelial differentiation and repair, Int. J. Mol. Sci. 23 (2022), https://doi.org/10.3390/ijms232113064.
[50] A.E. Vaughan, A.N. Brumwell, Y. Xi, J.E. Gotts, D.G. Brownfield, B. Treutlein, K. Tan, V. Tan, F.C. Liu, M.R. Looney, M.A. Matthay, J.R. Rock, H.A. Chapman, Lineage-negative progenitors mobilize to regenerate lung epithelium after major injury, Nature 517 (2015) 621–625, https://doi.org/10.1038/nature14112.
[51] W. Zuo, T. Zhang, D.Z. Wu, S.P. Guan, A.A. Liew, Y. Yamamoto, X. Wang, S.J. Lim, M. Vincent, M. Lessard, C.P. Crum, W. Xian, F. McKeon, p63(+)Krt5(+) distal airway stem cells are essential for lung regeneration, Nature 517 (2015) 616–620, https://doi.org/10.1038/nature13903.
[52] L. Yang, H. Xia, K. Smith, A. Gilbertsen, D. Beisang, J. Kuo, P.B. Bitterman, C. A. Henke, A CD44/Brg1 nuclear complex confers mesenchymal progenitor cells with enhanced fibrogenicity in idiopathic pulmonary fibrosis, JCI Insight 6 (2021), https://doi.org/10.1172/jci.insight.144652.
[53] M. Presta, E. Foglio, A. Churruca Schuind, R. Ronca, Long pentraxin-3 modulates the angiogenic activity of fibroblast growth Factor-2, Front. Immunol. 9 (2018), 2327, https://doi.org/10.3389/fimmu.2018.02327.
[54] M. Camozzi, S. Zacchigna, M. Rusnati, D. Coltrini, G. Ramirez-Correa, B. Bottazzi, A. Mantovani, M. Giacca, M. Presta, Pentraxin 3 inhibits fibroblast growth factor 2-dependent activation of smooth muscle cells in vitro and neointima formation in vivo, Arterioscler. Thromb. Vasc. Biol. 25 (2005) 1837–1842, https://doi.org/10.1161/01.ATV.0000177807.54959.7d.
[55] J. Hou, J. Shi, L. Chen, Z. Lv, X. Chen, H. Cao, Z. Xiang, X. Han, M2 macrophages promote myofibroblast differentiation of LR-MSCs and are associated with pulmonary fibrogenesis, Cell Commun. Signal 16 (2018), 89, https://doi.org/10.1186/s12964-018-0300-8.
[56] W.J. Ji, Y.Q. Ma, X. Zhou, Y.D. Zhang, R.Y. Lu, H.Y. Sun, Z.Z. Guo, Z. Zhang, Y. M. Li, L.Q. Wei, Temporal and spatial characterization of mononuclear phagocytes in circulating, lung alveolar and interstitial compartments in a mouse model of bleomycin-induced pulmonary injury, J. Immunol. Methods 403 (2014) 7–16, https://doi.org/10.1016/j.jim.2013.11.012.
[57] L. Lis-Lopez, C. Bauset, M. Seco-Cervera, J. Cosin-Roger, Is the macrophage phenotype determinant for fibrosis development? Biomedicines 9 (2021) https://doi.org/10.3390/biomedicines9121747.
[58] L. Meziani, M. Mondini, B. Petit, A. Boissonnas, V. Thomas de Montpreville, O. Mercier, M.C. Vozenin, E. Deutsch, CSF1R inhibition prevents radiation pulmonary fibrosis by depletion of interstitial macrophages, Eur. Respir. J. 51 (2018), https://doi.org/10.1183/13993003.02120-2017.
[59] A. Shiraki, N. Kotooka, H. Komoda, T. Hirase, J.I. Oyama, K. Node, Pentraxin-3 regulates the inflammatory activity of macrophages, Biochem Biophys. Rep. 5 (2016) 290–295, https://doi.org/10.1016/j.bbrep.2016.01.009.
[60] C. Overed-Sayer, E. Miranda, R. Dunmore, E. Liarte Marin, L. Beloki, D. Rassl, H. Parfrey, A. Carruthers, A. Chahboub, S. Koch, G. Guler-Gane, M. Kuziora, A. Lewis, L. Murray, R. May, D. Clarke, Inhibition of mast cells: a novel mechanism by which nintedanib may elicit anti-fibrotic effects, Thorax 75 (2020) 754–763, https://doi.org/10.1136/thoraxjnl-2019-214000.
[61] C. Shimbori, C. Upagupta, P.S. Bellaye, E.A. Ayaub, S. Sato, T. Yanagihara, Q. Zhou, A. Ognjanovic, K. Ask, J. Gauldie, P. Forsythe, M.R.J. Kolb, Mechanical stress-induced mast cell degranulation activates TGF-beta1 signalling pathway in pulmonary fibrosis, Thorax 74 (2019) 455–465, https://doi.org/10.1136/thoraxjnl-2018-211516.
[62] D.D. Metcalfe, D. Baram, Y.A. Mekori, Mast cells, Physiol. Rev. 77 (1997) 1033–1079, https://doi.org/10.1152/physrev.1997.77.4.1033.
[63] L. Deng, T. Huang, L. Zhang, T cells in idiopathic pulmonary fibrosis: crucial but controversial, Cell Death Discov. 9 (2023), 62, https://doi.org/10.1038/s41420-023-01344-x.
[64] L. Lei, C. Zhao, F. Qin, Z.Y. He, X. Wang, X.N. Zhong, Th17 cells and IL-17 promote the skin and lung inflammation and fibrosis process in a bleomycin-induced murine model of systemic sclerosis, Clin. Exp. Rheuma 34 (Suppl 100) (2016) 14–22.
[65] S. Lo Re, M. Lecocq, F. Uwambayinema, Y. Yakoub, M. Delos, J.B. Demoulin, S. Lucas, T. Sparwasser, J.C. Renauld, D. Lison, F. Huaux, Platelet-derived growth factor-producing CD4+ Foxp3+ regulatory T lymphocytes promote lung fibrosis, Am. J. Respir. Crit. Care Med 184 (2011) 1270–1281, https://doi.org/10.1164/rccm.201103-0516OC.
[66] X. Peng, M.W. Moore, H. Peng, H. Sun, Y. Gan, R.J. Homer, E.L. Herzog, CD4+ CD25+FoxP3+ Regulatory Tregs inhibit fibrocyte recruitment and fibrosis via suppression of FGF-9 production in the TGF-beta1 exposed murine lung, Front Pharm. 5 (2014) 80, https://doi.org/10.3389/fphar.2014.00080.
[67] C. Prior, P.L. Haslam, In vivo levels and in vitro production of interferon-gamma in fibrosing interstitial lung diseases, Clin. Exp. Immunol. 88 (1992) 280–287, https://doi.org/10.1111/j.1365-2249.1992.tb03074.x.
[68] R.A. Reilkoff, H. Peng, L.A. Murray, X. Peng, T. Russell, R. Montgomery, C. Feghali-Bostwick, A. Shaw, R.J. Homer, M. Gulati, A. Mathur, J.A. Elias, E.L. Herzog, Semaphorin 7a+ regulatory T cells are associated with progressive idiopathic pulmonary fibrosis and are implicated in transforming growth factor-beta1-induced pulmonary fibrosis, Am. J. Respir. Crit. Care Med. 187 (2013) 180–188, https://doi.org/10.1164/rccm.201206-1109OC.
[69] A. Saito, H. Okazaki, I. Sugawara, K. Yamamoto, H. Takizawa, Potential action of IL-4 and IL-13 as fibrogenic factors on lung fibroblasts in vitro, Int. Arch. Allergy Immunol. 132 (2003) 168–176, https://doi.org/10.1159/000073718.
[70] Z. Daniil, P. Kitsanta, G. Kapotsis, M. Mathioudaki, A. Kollintza, M. Karatza, J. Milic-Emili, C. Roussos, S.A. Papiris, CD8+ T lymphocytes in lung tissue from patients with idiopathic pulmonary fibrosis, Respir. Res 6 (2005), 81, https://doi.org/10.1186/1465-9921-6-81.
[71] T.Y. Brodeur, T.E. Robidoux, J.S. Weinstein, J. Craft, S.L. Swain, A. Marshak-Rothstein, IL-21 promotes pulmonary fibrosis through the induction of profibrotic CD8+ T cells, J. Immunol. 195 (2015) 5251–5260, https://doi.org/10.4049/jimmunol.1500777.
[72] M. Croft, L. Carter, S.L. Swain, R.W. Dutton, Generation of polarized antigen-specific CD8 effector populations: reciprocal action of interleukin (IL)-4 and IL-12

in promoting type 2 versus type 1 cytokine profiles, J. Exp. Med 180 (1994) 1715–1728, https://doi.org/10.1084/jem.180.5.1715.
[73] P. Baruah, A. Propato, I.E. Dumitriu, P. Rovere-Querini, V. Russo, R. Fontana, D. Accapezzato, G. Peri, A. Mantovani, V. Barnaba, A.A. Manfredi, The pattern recognition receptor PTX3 is recruited at the synapse between dying and dendritic cells, and edits the cross-presentation of self, viral, and tumor antigens, Blood 107 (2006) 151–158, https://doi.org/10.1182/blood-2005-03-1112.
[74] M. Lech, C. Rommele, O.P. Kulkarni, H.E. Susanti, A. Migliorini, C. Garlanda, A. Mantovani, H.J. Anders, Lack of the long pentraxin PTX3 promotes autoimmune lung disease but not glomerulonephritis in murine systemic lupus erythematosus, PLoS One 6 (2011), e20118, https://doi.org/10.1371/journal.pone.0020118.
[75] G. Gupta, Z. Mou, P. Jia, R. Sharma, R. Zayats, S.M. Viana, L. Shan, A. Barral, V. S. Boaventura, T.T. Murooka, A. Soussi-Gounni, C.I. de Oliveira, J.E. Uzonna, The Long Pentraxin 3 (PTX3) Suppresses Immunity to Cutaneous Leishmaniasis by Regulating CD4(+) T Helper Cell Response, Cell Rep. 33 (2020), 108513, https://doi.org/10.1016/j.celrep.2020.108513.
[76] S. Lo Re, D. Lison, F. Huaux, CD4+ T lymphocytes in lung fibrosis: diverse subsets, diverse functions, J. Leukoc. Biol. 93 (2013) 499–510, https://doi.org/10.1189/jlb.0512261.
[77] L. Richeldi, H.R. Collard, M.G. Jones, Idiopathic pulmonary fibrosis, Lancet 389 (2017) 1941–1952, https://doi.org/10.1016/S0140-6736(17)30866-8.
[78] Y. Xu, T. Mizuno, A. Sridharan, Y. Du, M. Guo, J. Tang, K.A. Wikenheiser-Brokamp, A.T. Perl, V.A. Funari, J.J. Gokey, B.R. Stripp, J.A. Whitsett, Single-cell RNA sequencing identifies diverse roles of epithelial cells in idiopathic pulmonary fibrosis, JCI Insight 1 (2016), e90558, https://doi.org/10.1172/jci.insight.90558.
[79] J.K. Ochieng, K. Schilders, H. Kool, A. Boerema-De Munck, M. Buscop-Van Kempen, C. Gontan, R. Smits, F.G. Grosveld, R.M. Wijnen, D. Tibboel, R.J. Rottier, Sox2 regulates the emergence of lung basal cells by directly activating the transcription of Trp63, Am. J. Respir. Cell Mol. Biol. 51 (2014) 311–322, https://doi.org/10.1165/rcmb.2013-0419OC.
[80] D. Petukhov, M. Richter-Dayan, Z. Fridlender, R. Breuer, S.B. Wallach-Dayan, Increased regeneration following stress-induced lung injury in bleomycin-treated chimeric mice with CD44 knockout mesenchymal cells, Cells 8 (2019), https://doi.org/10.3390/cells8101211.
[81] U. Smole, B. Kratzer, W.F. Pickl, Soluble pattern recognition molecules: Guardians and regulators of homeostasis at airway mucosal surfaces, Eur. J. Immunol. 50 (2020) 624–642, https://doi.org/10.1002/eji.201847811.
[82] J.Y. Chi, Y.W. Hsiao, H.Y. Liang, T.H. Huang, F.W. Chen, C.Y. Chen, C.Y. Ko, C. C. Cheng, J.M. Wang, Blockade of the pentraxin 3/CD44 interaction attenuates lung injury-induced fibrosis, Clin. Transl. Med 12 (2022), e1099, https://doi.org/10.1002/ctm2.1099.
[83] M. Garcia-Rojo, J. Sanchez, E. de la Santa, E. Duran, J.L. Ruiz, A. Silva, F.J. Rubio, A.M. Rodriguez, B. Melendez, L. Gonzalez, B. Lopez-Viedma, Automated image analysis in the study of lymphocyte subpopulation in eosinophilic oesophagitis, Diagn. Pathol. 9 (Suppl 1) (2014), S7, https://doi.org/10.1186/1746-1596-9-S1-S7.
[84] T. Annese, R. Tamma, M. Bozza, A. Zito, D. Ribatti, Autocrine/paracrine loop between SCF(+)/c-Kit(+) mast cells promotes cutaneous melanoma progression, Front Immunol. 13 (2022), 794974, https://doi.org/10.3389/fimmu.2022.794974.
[85] S.A. Papiris, A. Kollintza, P. Kitsanta, G. Kapotsis, M. Karatza, J. Milic-Emili, C. Roussos, Z. Daniil, Relationship of BAL and lung tissue CD4+ and CD8+ T lymphocytes, and their ratio in idiopathic pulmonary fibrosis, Chest 128 (2005) 2971–2977, https://doi.org/10.1378/chest.128.4.2971.
[86] L. Qin, W.Z. Wang, H.R. Liu, W.B. Xu, M.W. Qin, Z.H. Zhang, Y. Xiao, W.J. Zhen, J. H. Shi, CD4+ and CD8+ T lymphocytes in lung tissue of NSIP: correlation with T lymphocytes in BALF, Respir. Med 107 (2013) 120–127, https://doi.org/10.1016/j.rmed.2012.09.021.
[87] B.B. Moore, C.M. Hogaboam, Murine models of pulmonary fibrosis, Am. J. Physiol. Lung Cell Mol. Physiol. 294 (2008) L152–160, https://doi.org/10.1152/ajplung.00313.2007.
[88] T. Kishaba, Evaluation and management of idiopathic pulmonary fibrosis, Respir. Invest. 57 (2019) 300–311, https://doi.org/10.1016/j.resinv.2019.02.003.